

Ultra-efficient superconducting Dayem bridge field-effect transistor

Federico Paolucci,^{*,†} Giorgio De Simoni,[†] Elia Strambini,[†] Paolo Solinas,[‡] and Francesco Giazotto[†]

[†]*NEST, Istituto Nanoscienze-CNR and Scuola Normale Superiore, I-56127 Pisa, Italy*
[‡]*SPIN-CNR, Via Dodecaneso 33, I-16146 Genova, Italy*

E-mail: federico.paolucci@nano.cnr.it

Abstract

Superconducting field-effect transistor (*SuFET*) and Josephson field-effect transistor (*JoFET*) technologies take advantage of electric field induced control of charge carrier concentration in order to modulate the channel superconducting properties. Despite field-effect is believed to be unaffactive for superconducting metals, recent experiments showed electric field dependent modulation of the critical current (I_C) in a fully metallic transistor. Yet, the grounding mechanism of this phenomenon is not completely understood. Here, we show the experimental realization of Ti-based Dayem bridge field-effect transistors (*DB – FETs*) able to control I_C of the superconducting channel. Our easy fabrication process *DB – FETs* show symmetric full suppression of I_C for an applied critical gate voltage as low as $V_G^C \simeq \pm 8V$ at temperatures reaching about the 85% of the record critical temperature $T_C \simeq 550mK$ for titanium. The gate-independent T_C and normal state resistance (R_N) coupled with the increase of resistance in the superconducting state (R_S) for gate voltages close to the critical value (V_G^C) suggest the creation of field-effect induced metallic puddles in the superconducting sea. Our devices show extremely high values of transconductance ($|g_m^{MAX}| \simeq 15\mu A/V$ at $V_G \simeq \pm 6.5V$) and variations of Josephson kinetic inductance (L_K) with V_G of two orders of magnitude. Therefore, the *DB – FET* appears as an ideal candidate for the realization of superconducting electronics, superconducting qubits, tunable interferometers as well as photon detectors.

Conventional computation is hinged on the use of field-effect transistors (*FETs*)^{1,2} based on complementary metal-oxide-semiconductor (*CMOS*) technology.³ Semiconductor-based electronics suffers from dissipation caused by charging and de-charging the gate capacitors, and by the current flowing through the *FET* channel.⁴ The latter can be eliminated by employing a class of devices where a high critical temperature (T_C) superconductor thin film sub-

stitutes the semiconducting channel: the superconducting field-effect transistor (*SuFET*).⁵ By applying a gate voltage (V_G) the charge carrier concentration in the channel can be controlled (because of their low intrinsic carrier density) and, as a consequence, the normal state resistance (R_N), the superconducting critical temperature^{6,7} and the critical current (I_C) are modulated.^{8,9} A similar approach consists in employing superconducting source and

drain electrodes which induce Cooper pairs flowing in a semiconducting channel through the so-called superconducting proximity effect.¹⁰ In the resulting device, called Josephson field-effect transistor (*JoFET*),¹¹ T_C and I_C can be controlled via field-effect modulation of the carrier concentration of the semiconductor.^{12,13} Since the first demonstration of Josephson supercurrent in proximized semiconductor nanowires,¹⁴⁻¹⁶ 1D channels have been implemented in *JoFET* technology,^{17,18} too. This gave rise to novel experiments shedding light on long standing physics open problems, such as Majorana bound states,^{19,20} and developing new superconductor-based qubit technologies.²¹⁻²³ Despite field-effect is believed to be unaffactive on conventional superconducting metals, recent experiments showed full suppression of supercurrent in all-metallic transistors based on different Bardeen-Cooper-Schrieffer (*BCS*) wires made of aluminum and titanium.²⁴ This discovery could pave the way to the realization of novel all-metallic gate-tunable devices, such as "gatemons",²¹⁻²³ interferometers,²⁵ Josephson parametric amplifiers^{26,27} and photon detectors,²⁸ that could take advantage of a simple single-step fabrication and scalable technology.

Here, we report the realization of the first fully metallic Dayem bridge field-effect transistors (*DB-FETs*). Remarkably, our titanium-based devices show an unprecedented superconducting critical temperature $T_C \sim 540\text{mK}$ for Ti,²⁹⁻³¹ and a symmetric complete suppression of the supercurrent for voltages applied to the lateral gate electrodes as large as $\pm 8\text{V}$. Furthermore, the *DB-FETs* exhibit values of transconductance reaching $15\mu\text{A}/\text{V}$ at about $\pm 6.5\text{V}$ and variations of two order of magnitude in the Josephson kinetic inductance (L_K) with the applied V_G .

The structure of a typical Dayem bridge field-effect transistor is shown in Figure 1a. The *DB-FET* consists of a $4\mu\text{m}$ wide titanium (Ti) thin film (of thickness $\sim 30\text{nm}$) interrupted by a $\sim 125\text{-nm}$ -long and $\sim 300\text{-nm}$ -wide constriction. In correspondence of the constriction, at a distance of about $120 - 150\text{nm}$, two side electrodes (green stripes in Figure 1a) al-

low to apply an electrostatic field on the bridge region. The devices were realized by a single-step electron beam lithography and evaporation of titanium onto a p^{++} -doped silicon (Si) commercial wafer covered by 300nm of silicon dioxide (SiO_2). The 30-nm -thick Ti layers were deposited at room temperature in an ultra-high vacuum electron beam evaporator (base pressure $\sim 10^{-11}\text{Torr}$) at a deposition rate ranging from 10 to $13\text{\AA}/\text{s}$. The electrical characterization of the *DB-FETs* was performed by standard four wire technique in a filtered He^3 - He^4 dry dilution refrigerator at different bath temperatures (in the range $40\text{mK} - 550\text{mK}$). Both resistance vs temperature and resistance vs magnetic field characteristics were obtained by low frequency lock-in technique, while the current vs voltage behaviors were carried out by applying a low-noise current bias and measuring the voltage drop by a room-temperature differential preamplifier. Finally, the gate voltage was applied by a low-noise source-measurement-unit.

Our Dayem bridges show an unprecedented critical temperature for titanium $T_C \sim 540\text{mK}$ ²⁹⁻³¹ (see the resistance vs temperature trace depicted by the green line in Figure 1b) corresponding to a *BCS* zero-temperature superconducting energy gap $\Delta_0 = 1.764k_B T_C \simeq 82\mu\text{eV}$, where k_B is the Boltzmann constant. On the other hand, our *DB-FETs* exhibit typically a critical perpendicular-to-plane magnetic field of $\sim 115\text{mT}$, as displayed by the blue line of Figure 1b. In order to investigate the dissipationless Cooper pairs transport, we measured the $I - V$ characteristics of our devices as a function of bath temperature (T). A set of $I - V$ characteristics at selected temperatures is represented in Figure 1c. The superconducting critical current reaches a value $I_C \simeq 30\mu\text{A}$ almost constant for temperatures lower than $\sim 125\text{mK}$ and monotonically decreases for higher temperature, as shown in Figure 1d. The transistor $I - V$ characteristics are hysteretic due to heating induced in the sample while switching from the normal to the superconducting state.³² In particular, the switching current from the resistive to the dissipationless state, known as retrapping cur-

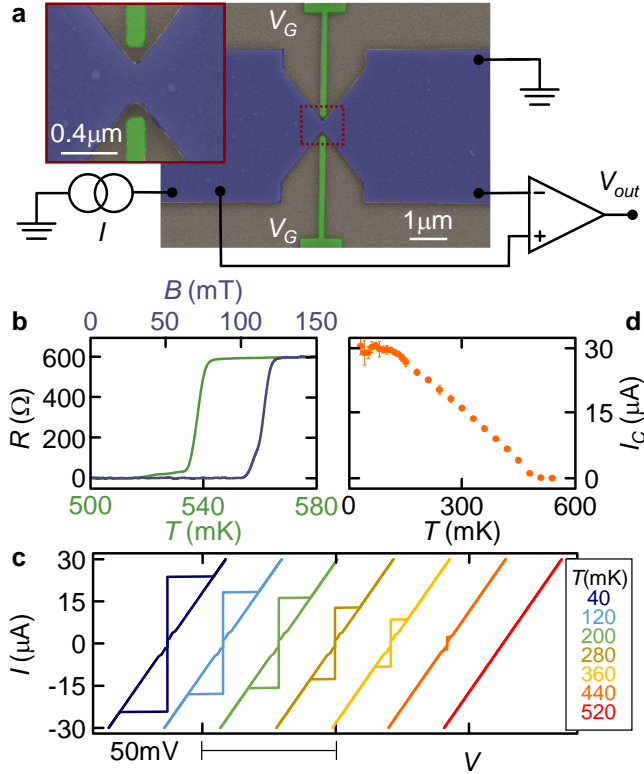


Figure 1: (a) False color electron micrograph of a typical Ti-based Dayem bridge transistor. The Josephson junction (blue) is current biased and the voltage drop is measured with a room temperature voltage amplifier, while the gate voltage is applied to both gate electrodes (green fingers). The inset shows a blow-up of the core of the device. (b) Resistance R as a function of temperature T (green line, bottom horizontal axis), and R vs perpendicular-to-plane magnetic field B at 50mK (blue line, top horizontal axis) characteristics of the $DB - FET$. The normal-state resistance of the device is about 600Ω . (c) Back and forth current I vs voltage V characteristics of a typical $DB - FET$ measured at different temperatures. The curves are horizontally offset by 20 mV for clarity. (d) Full temperature evolution of the critical current I_C . The error bars represent the standard deviation of I_C calculated over 50 repetitions.

rent, is almost constant ($I_R \simeq 1.6\mu A$) in the complete temperature range.

To demonstrate the field-effect performances of the $DB - FET$, we carried out $I - V$ measurements for different values of gate voltage. In our experiments we applied the same value of V_G to both gate electrodes to maximize the impact of the electric field on the supercurrent. As shown in Figure 2a for sample A, the critical current I_C monotonically decreases with the applied gate voltage until reaching full suppression. On the other hand, the retrapping current (I_R) remains constant until $I_C > I_R$, while by further increasing V_G the switching and retrapping currents assume the same value ($I_R = I_C$). Remarkably, the suppression of I_C is symmetric with the sign of V_G (*bipolar* field-effect) and the

normal state resistance (R_N) of the $DB - FET$ is unaffected by the electric field (see the constant slope of the $I - V$ curves in Figure 2a). This is in stark contrast with $SuFETs$ ⁵⁻⁹ and $JoFETs$.¹²⁻¹⁶ As a consequence, charge depletion of the Josephson transistor channel can not account for the I_C reduction.

In order to study the complete behavior of the $DB - FETs$ we measured I_C as a function of the applied gate voltage at different bath temperatures ranging from 50mK to 450mK. By normalizing the critical current with respect to its value in the absence of any applied gate bias [$I_C(V_G)/I_C(0)$], it is possible to directly compare the behavior of different devices, as shown in Figure 2b, even if their intrinsic critical current is different [$I_C(T = 50mK) \simeq 28\mu A$ for

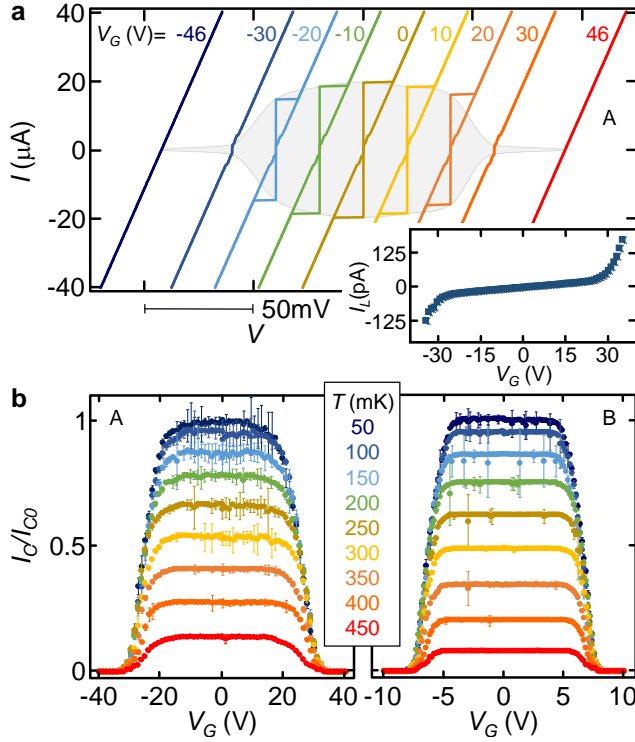


Figure 2: (a) Back and forth current I vs voltage V characteristics of sample A measured at 50mK for several values of gate voltage V_G . The curves are horizontally offset proportionally to V_G for clarity. The semi-transparent area depicts the parameters space where superconductivity persists. The inset shows the leakage current measured in our setup I_L as a function of gate voltage V_G . (b) Normalized critical current I_C/I_{C0} as a function of gate voltage V_G measured at different bath temperatures T for two $DB-FET$ (*i.e.*, samples A and B). The error bars represent the standard deviation of I_C calculated over 50 repetitions.

sample A and $I_C(T = 50\text{mK}) \simeq 24\mu\text{A}$ for sample B]. The critical current of the two devices shows a qualitatively similar behavior both with gate voltage and temperature. In particular, at $T = 50\text{mK}$ the critical current remains constant by increasing V_G , then it starts to decrease until its full suppression ($I_C = 0$) by further rising the gate voltage. For higher values of the temperature the maximum value of critical current lowers, and, on the one hand, the plateau of constant I_C widens in V_G while, on the other hand, the foot of the transition (*i.e.*, the first value of V_G giving $I_C = 0$) remains constant at temperatures up to $\sim 85\%T_C$ (see Figure 2b). This behavior resembles the recent results obtained on gated BCS Ti and Al wires and thin films.²⁴ From a quantitative point of view, the main difference between sample A and B resides in the gate voltage operation ranges (see Figure 2b). Sample A exhibits complete suppression of the critical current at a

critical voltage $V_G^C \simeq \pm 32\text{V}$, whereas sample B shows an extraordinary low critical voltage of about $\pm 8\text{V}$. The latter impressive value of V_G^C is comparable to the gate voltages employed in $CMOS$ technology ($V_{dd} = 5\text{V}$), and it can be attributed to the lower distance between the constriction (active element) and the gate electrodes in sample B .

In addition, during all experiments we have carefully monitored the leakage current I_L of the entire measurement circuit while applying the gate voltage V_G (see the inset of Figure 2a). The leakage current is always of the order of tens of pA ($I_L \sim 10^{-6}I_C(V_G = 0)$). In particular, for $V_G = 25\text{V}$ the critical current suppression is $\sim 13\mu\text{A}$ while $I_L \simeq 20\text{pA}$ (with a resulting gate resistance $R_G \simeq 1.25\text{T}\Omega$). In order to exclude any quasiparticle overheating due to direct injection of a portion of I_L as source of the supercurrent suppression we recorded the temperature dependence of the resistance (R)

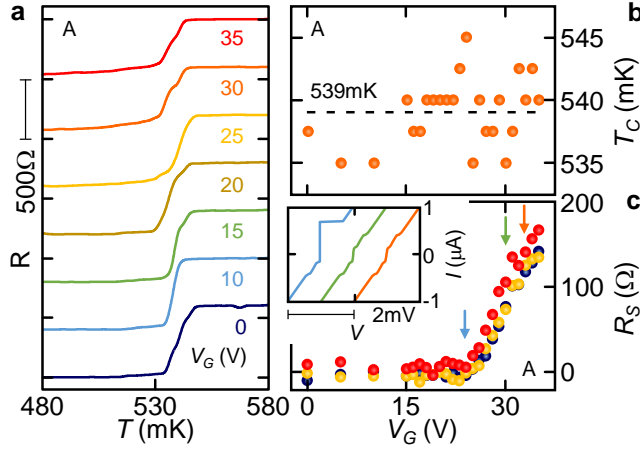


Figure 3: (a) Resistance R as a function of temperature T measured on sample A for different values of gate voltage V_G . The curves are vertically offset for clarity. (b) Extracted values of critical temperature T_C as a function of gate voltage V_G for sample A . The average critical temperature $T_C = 539$ mK is shown. (c) Zero-bias resistance in the superconducting state R_S as a function of V_G measured on sample A for $T = 480$ mK (blue), 500 mK (yellow) and 520 mK (red). The inset shows the $I - V$ characteristics at $T_{bath} = 50$ mK for values of gate voltage indicated by the colored arrows.

of our $DB - FETs$ as a function of the applied gate voltage (see Figure 3a). Any heat injection able to suppress the critical current would, at the same time, result in a measurable reduction of the critical temperature.³³ In our Dayem bridge transistors, T_C remains constant (within the experimental error due to temperature stabilization) over the complete range of applied gate voltages, as shown for sample A in Figure 3b. For instance, by applying a gate voltage $V_G = 25$ V a reduction of 80% in I_C is measured while the critical temperature is completely unaffected. Analogously, the normal state resistance is not influenced by the gate voltage and shows an electric field independent value $R_N \simeq 600 \Omega$ comparable with the values extracted from the $I - V$ characteristics.

A careful analysis of the R vs T data highlights that the resistance in the superconducting state (R_S) near full suppression of the supercurrent strongly depends on V_G , as shown in Figure 3c. Specifically, a resistive component in the $I - V$ characteristics around zero bias appears and grows by rising the gate voltage. This phenomenology seems compatible with the creation of an inhomogeneous mixed state composed of normal metal and superconducting puddles. In this view, the superconducting ar-

eas maintain the same critical temperature of pristine Ti, while the dissipative parts interrupt the supercurrent flow providing the measured resistive component. The latter can be also noticed by zooming the $I - V$ curves obtained for values of gate voltage approaching V_G^C : a finite slope builds up (*i.e.*, a finite conductance, see the inset of Figure 3c) in correspondence of the dissipative component revealed by the R vs T experiments.

The standard figure of merit providing information about the performances of field-effect transistors is the transconductance. In superconductor-based devices, it is defined as $g_m = dI_C/dV_G$, *i.e.* the variation of the critical current with gate voltage. Figure 4a shows the behavior of g_m as a function of V_G measured at different temperatures for sample A . As expected, the transconductance shows different sign for $V_G < 0$ and $V_G > 0$ (given the suppression of I_C for both gate voltage polarities) since the numerical derivative is performed from negative to positive values of V_G . The strong temperature dependence of g_m is highlighted by plotting the absolute value of its maximum $|g_m^{MAX}|$ vs T , as depicted in the inset of Figure 4a for both sample A and B . In particular, g_m^{MAX} has an almost constant value

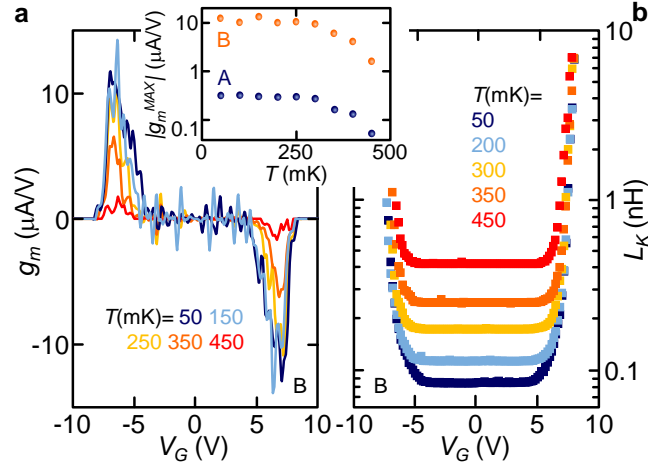


Figure 4: (a) Transconductance g_m as a function of gate voltage V_G for different values of temperature T measured on sample B. The inset shows the absolute value of the maximum of transconductance $|g_m^{\text{MAX}}|$ vs temperature T for devices A and B. (b) Kinetic inductance L_K as a function of gate voltage V_G for different values of temperature T measured on sample B.

($\sim 330\text{nA/V}$ at $V_G \simeq \pm 23\text{V}$ for sample A and $\sim 15\mu\text{A/V}$ at $V_G \simeq \pm 6.5\text{V}$ for sample B) up to $T \simeq T_C/2$, and by further rising the temperature it decreases by about one order of magnitude. The maximum value of the transconductance of our *DB-FETs* is comparable to that obtained on InAs thin films based *JoFETs* ($14\mu\text{A/V}$ at $V_G = 0.7\text{V}$ ¹³) and several orders of magnitude larger than that of semiconductor nanowire-based devices (a few nS at values of V_G of the order of several tens of volt¹⁴).

In our *DB-FETs*, the gate-dependent suppression of the critical current yields to an increase of the Josephson kinetic inductance, defined as $L_K = \hbar/(2eI_C)$ ³⁴ where \hbar is the reduced Planck constant and e is the electron charge, as shown in Figure 4b for different temperatures. In particular, the maximum value of L_K in our transistors is $\sim 8\text{nH}$, while its variation ranges from $\sim 10^{-13}\text{H}$ to $\sim 10^{-8}\text{H}$. Therefore, our *DB-FETs* seem suitable candidates for the realization of fully metallic superconducting qubits²¹⁻²³ and Josephson parametric amplifiers.^{26,27}

In conclusion, we have realized the first fully metallic Dayem bridge Josephson field-effect transistors allowing to control the critical current by applying a gate voltage. The simple fabrication single-step process elects the *DB-FET* as ideal candidate for a number of technological applications. Notably, our Ti

thin films showed a record critical temperature $T_C \sim 540\text{mK}$ for this superconducting metal. On the one hand, the *DB-FETs* allow a bipolar fine control of the critical current until its full suppression for values of gate voltage of $\sim \pm 8\text{V}$. On the other hand, differently from conventional *JoFETs*, the critical temperature and the normal state resistance of the transistors are not affected by an electric field. The constant T_C and the change of R_S with V_G suggest the creation of electric field induced inhomogeneous state in the superconductor consisting of metallic puddles. Furthermore, the *DB-FETs* exhibit very high values of transconductance ($|g_m^{\text{MAX}}| \simeq 15\mu\text{A/V}$ at $V_G \simeq \pm 6.5\text{V}$) and variations of Josephson kinetic inductance of two orders of magnitude. Therefore, the metallic Dayem bridge Josephson field-effect transistors are excellent candidates for the realization of "gatemons",²¹⁻²³ parametric amplifiers,^{26,27} tunable interferometers²⁵ and photon detectors.²⁸

Author Contributions

F.P. and G.D.S. fabricated the samples and performed the experiments. F.P. and G.D.S. analysed the data with inputs from E.S., P.S. and F.G. F.G. conceived the the experiment. F.P. wrote the manuscript with inputs from all the

authors. All the authors discussed the results and their implications equally.

Acknowledgement The authors acknowledge the European Research Council under the European Unions Seventh Framework Programme (FP7/2007-2013)/ERC Grant No. 615187 - COMANCHE, the European Union (FP7/2007-2013)/REA Grant No. 630925 - COHEAT and the MIUR under the FIRB2013 Project Coca (Grant No. RBFR1379UX) for partial financial support. The work of G.D.S. and F.P. was funded by Tuscany Region under the FARFAS 2014 project SCIADRO. The work of E.S. is funded by a Marie Curie Individual Fellowship (MSCA-IFEF-ST No. 660532-SuperMag).

References

- (1) Lilienfeld, J. E. Method and apparatus for controlling electric currents. U.S. Patent 1,745,175A, Oct. 8, 1926.
- (2) Nishizawa, J-I. Junction Filed-Effect Devices. In *Semiconductor Devices for Power Conditioning*; Sittig, R., Roggwiller, P., Eds.; Earlier Brown Boveri Symposia; Springer, Boston, MA, 1982; pp 241-272.
- (3) Wanlass, F. Low stad-by power complementary field effect circuitry. U.S. Patent 3,356,858, Dec. 5, 1967.
- (4) Tolpygo, S. K. *Low Temp. Phys.* **2016**, 42, 361.
- (5) Nishino, T.; Hatano, M.; Hasegawa, H.; Murai, F.; Kure, T.; Hiraiwa, A.; Yagi, K.; Kawabe, U. *IEEE Trans. Electron Devices* **1989**, 10, 61.
- (6) Fiory, A. T.; Herbard, A. F.; Eick, R. H.; Mankiewich, P. M.; Howard, R. E.; O'Malley, M. L. *Phys. Rev. Lett.* **1990**, 65, 3441.
- (7) Mannhart, J.; Ströbel, J.; Bednorz, J. G.; Gerber, Ch. *Appl. Phys. Lett* **1993**, 62, 630.
- (8) Okamoto, M. *IEEE Trans. Electron Devices* **1992**, 39, 1661.
- (9) Mannhart, J.; Bednorz, J. G.; Müller, K. A.; Schlom, D. G.; Ströbel, J. *J. Alloys Compd.* **1993**, 195, 519.
- (10) Holm, R; Meissner, W. *Z. Phys.* **1932**, 74, 715.
- (11) Clark, T. D.; Prance, R. J.; Grassie, A. D. C. *J. Appl. Phys.* **1980**, 51, 2739.
- (12) Takayanagi, H.; Kawakami, T. *Phys. Rev. Lett.* **1985**, 54, 2449.
- (13) Akazaki, T.; Takayanagi, H.; Nitta, J.; Enoki, T. *Appl. Phys. Lett.* **1996**, 68, 418.
- (14) Doh, Y-J.; van Dam, J. A.; Roest, A. L.; Bakkers, E. P. A. M.; Kouwenhoven, L. P.; De Franceschi, S. *Science* **2005**, 309, 272.
- (15) Xiang, J.; Vidan, A.; Tinkham, M.; Westervelt, R. M.; Lieber, C. M. *Nanotechnol.* **2006**, 1, 208.
- (16) Paaajaste, J.; Amado, M.; Roddaro, S.; Bergeret, F. S.; Ercolani, D.; Sorba, L.; Giazotto, F. *Nano Lett.* **2015**, 15, 1803.
- (17) Jespersen, T. S.; Polianski, M. L.; Sørensen, C. B.; Flensberg, K.; Nygård, J. *New J. Phys.* **2009**, 11, 113025.
- (18) Abay, S.; Persson, D.; Nilsson, H.; Wu, F.; Xu, H. Q.; Fogelström, M.; Shumeiko, V.; Delsing, P. *Phys. Rev. B* **2014**, 89, 214508.
- (19) Mourik, V.; Zuo, K.; Frolov, S. M.; Plissard, S. R.; Bakkers, E. P. A. M.; Kouwenhoven, L. P. *Science* **2012**, 336, 1003.
- (20) Das, A.; Ronen, Y.; Most, Y.; Oreg, Y.; Heiblum, M.; Shtrikman, H. *Nat. Phys.* **2012**, 8, 887.
- (21) Larsen, T. W.; Petersson, K. D.; Kuemmeth, F.; Jespersen, T. S.; Krogstrup, P.; Nygård, J.; Marcus, C. M. *Phys. Rev. Lett.* **2015**, 115, 127001.

- (22) de Lange, G.; van Heck, B.; Bruno, A.; van Woerkom, D. J.; Geresdi, A.; Plissard, S. R.; Bakkers, E. P. A. M.; Akhmerov, A. R.; DiCarlo, L. *Phys. Rev. Lett.* **2015**, 115, 127002.
- (23) Casparis, L.; Larsen, T. W.; Olsen, M. S.; Kuemmeth, F.; Krogstrup, P.; Nygård, J.; Petersson, K. D.; Marcus, C. M. *Phys. Rev. Lett.* **2016**, 116, 150505.
- (24) De Simoni, G.; Paolucci, F.; Solinas, P.; Strambini, E.; Giazotto, F. *arXiv:1710.02400* **2018**.
- (25) Clarke, J.; Braginski, J. *The SQUID Handbook* VCH: New York, 2004.
- (26) Bergeal, N.; Schackert, F.; Metcalfe, M.; Vijay, R.; Manucharyan, V. E.; Frunzio, L.; Prober, D. E.; Schoelkopf, R. J.; Girvin, S. M.; Devoret, M. H. *Nature* **2010**, 465, 64.
- (27) Kamal, A.; Clarke, J.; Devoret, M. H. *Nat. Phys.* **2011**, 78, 311.
- (28) Gol'tsman, G. N.; Okunev, O.; Chulkova, G.; Semenov, A.; Smirnov, K.; Voronov, B.; Dzardanov, A. *Appl. Phys. Lett.* **2001**, 79, 705.
- (29) Peruzzi, A.; Gottardi, E.; Peroni, I.; Ponti, G.; Ventura, G. *Nucl. Phys. B* **1999**, 78, 576.
- (30) Tirelli, S.; Savin, A. M.; Pascual Garcia, C.; Pekola, J. P.; Beltram, F.; Giazotto, F. *Phys. Rev. Lett.* **2008**, 101, 077004.
- (31) Faivre, T.; Golubev, D.; Pekola, J. P. *J. Appl. Phys.* **2008**, 116, 094302.
- (32) Courtois, H.; Meschke, M.; Peltonen, J. T.; Pekola, J. P. *Phys. Rev. Lett.* **2008**, 101, 067002.
- (33) Morpurgo, A.; Klapwijk, T. M.; van Wees, B. J. *Appl. Phys. Lett.* **1998**, 72, 966.
- (34) Giazotto, F.; Heikkilä, T. T.; Pepe, G. P.; Heliö, P.; Luukanen, A.; Pekola, J. P. *Appl. Phys. Lett.* **2008**, 92, 162507.

Graphical TOC Entry

